CHAPTER 4
STOPE SUPPORT MODEL

4.1 INTRODUCTION TO THE SUPPORT MODEL

The rock engineering practitioner has at his disposal laboratory test press results for a range of various stope support types. The majority of these tests are done in a laboratory at a much faster rate of deformation as compared to the underground environment. The laboratory test rate is typically of the order of tenths of millimetres per minute while the underground closure rate is normally quasi-static and generally in the order of millimetres per day. The rate of deformation can be rapid during rockburst conditions, and typically in the order of metres or fractions of metres per second.

There is no facility in South Africa where a full sized pack can be tested at a dynamic rate of say 1 to 3 metres per second. The information that is available to the South African mining industry arrives from work done by Taggart (1996) and by Smit, Erasmus and Grobler (1998) at the test facility at the Materialprüfungsamt Nordrhein-Westfalen in Dortmund, Germany.

The load or deformation rate as well as the height of the support element have an influence on the performance of a support element. The stope width at which the support unit is installed can vary quite significantly from the height of the unit that was tested. This phenomenon does not only have an impact on the support performance of packs but also on the potential for buckling failure in the case of timber elongates. For purposes of design and analysis of stope support it is important that these factors be taken into consideration when assessing a support element.

The stope support model that is described in the thesis is developed with the aim to be available as a design tool that rock engineering practitioners can use to quantify the in-situ performance of stope support. The engineer must be able to do this for very specific underground conditions and for different support types.

For the support model to reflect the in-situ response of stope support, all factors that can potentially have an influence on its performance must be taken into consideration. The laboratory test results must therefore be adjusted to compensate for these.

The model can only be used as a design tool if the effects of height and loading rate can be quantified in engineering and mathematical terms and incorporated into the model. The support model is not intended to make provision for so-called human errors such as poor support construction, erratic support spacing or stope support that is not installed at all.

Case studies have been used to describe the performance of stope support in an attempt to understand and quantify support reaction and behaviour. Here the capacity of the stope support is compared to the support demand imposed on it by the rockmass. These are described in Chapter 6 of this document with case studies illustrating the application in Chapter 7.

4.2 METHODOLOGY ADOPTED FOR DEVELOPMENT OF MODEL

Laboratory test curves of stope support units can be compared to a seismogram that is recorded by a seismic network. Even though this information is of some use to the trained and experienced seismologist, the seismogram will just remain another waveform. It is only when the seismogram is "translated" and presented in a mathematical format through a Fourier transformation that it is of more use to the seismologist as end-user. The character of a seismic event can be determined by studying its source parameters through the analysis of the seismogram. This approach represents a way in which the behaviour of the rockmass is described in some mathematical "language" that can be interpreted and understood by the seismologist.

This is also true for test curves of various stope support elements. Even though an experienced rock engineer can obtain some information from a load-deformation curve, more analysis is required to be able to quantify the characteristics of the support unit. It is therefore essential that the load-deformation curve be "translated" into some "language" that does not only give a true reflection of the laboratory test result, but also enables the end-user to quantify its performance characteristics. This is possible through the application of a mathematical process similar to that of a seismogram.

The ideal mathematical process must be able to quantify the capacity of a support unit. The capacity of the support units in this context refers to the in-situ performance of such an element for a certain underground environment. The factors that influence its performance are also presented in a mathematical format and taken into consideration. The final (or combined) model is in a format that can be manipulated by the end user to

describe the character of the support element. It enables him to quantify the effect that various influences have on the performance of such a support unit. The end user has the option to change some of these parameters and quantify the effect that it has on the capacity of the support unit.

4.2.1 Mathematical representation of laboratory test results

A polynomial of the n^{th} order was applied to best describe the laboratory test curves of support units mathematically. The order of the polynomial is a function of the accuracy with which the curve is reproduced. The majority of the support elements were found to be best described by a sixth order polynomial.

The mathematical equation representing a support unit is in the format:

$$y = f(x) = c_1x^6 + c_2x^5 + c_3x^4 + c_4x^3 + c_5x^2 + c_6x \qquad (4.1)$$

where:

y = $f(x)$ = Load generated by element (kN);
x = Deformation (mm); and
c_n = Constants with n = 1,2 .....6.

Figure 4.1 shows a typical example of a laboratory test curve for a 75 cm x 75 cm Solid Hardgum Matpack, 1.8 m high that was tested at a rate of 14 mm/minute. The relatively good correlation that exists between the 6^{th} order polynomial representing the curve and the laboratory test press result is illustrated. The 6^{th} order polynomial that describes the mathematical fit shown in Figure 4.1 is:
$y = 759.66x^6 - 1636.4x^5 + 1306.8x^4 - 440.47x^3 + 40.768x^2 + 13.918x$.

This process was repeated for all the timber and concrete packs as well as timber elongates commonly used in the gold and platinum mining industry.

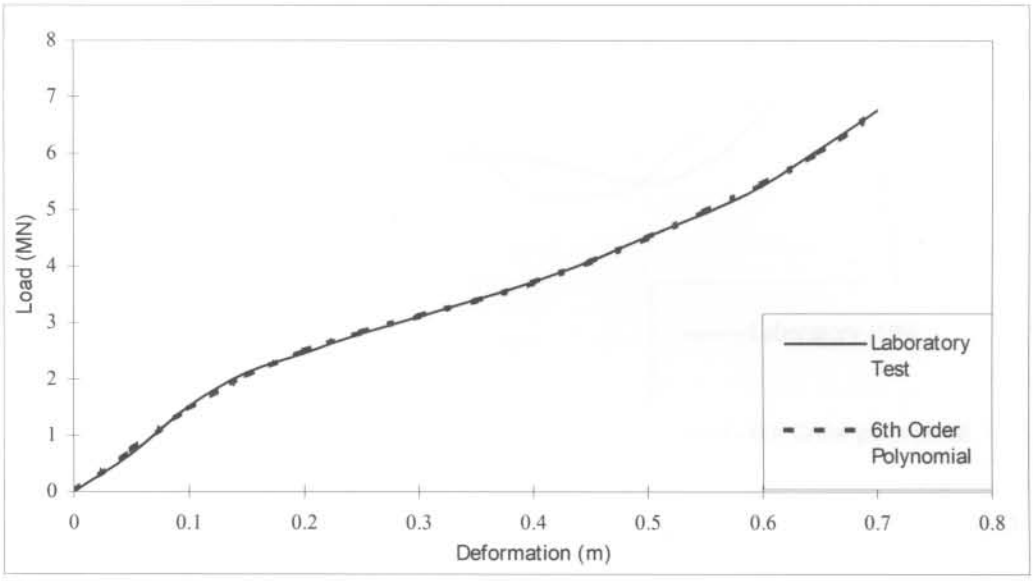

Figure 4.1: Laboratory test curve and the 6th order polynomial fit to the data for a 75 cm x 75 cm Solid Hard gum Matpack

Figure 4.2 shows the polynomial representation of a 200 mm diameter Wedge Prop, 2.0 m high and tested at a rate of 5 mm/minute. The polynomial equation was manipulated in cases where a perfect fit was not possible initially. The polynomial was altered so that the estimated energy over the total deformation range would be more or less the same as for the laboratory test curve.

A summary of all constants for the different support units that were analysed is given in Table 4.2 at the end of the chapter. The table shows all detail with respect to the type and dimensions of support as well as the rate of deformation during the laboratory test.

Graphs illustrating the polynomial fit to the laboratory data are included as Appendix 1.

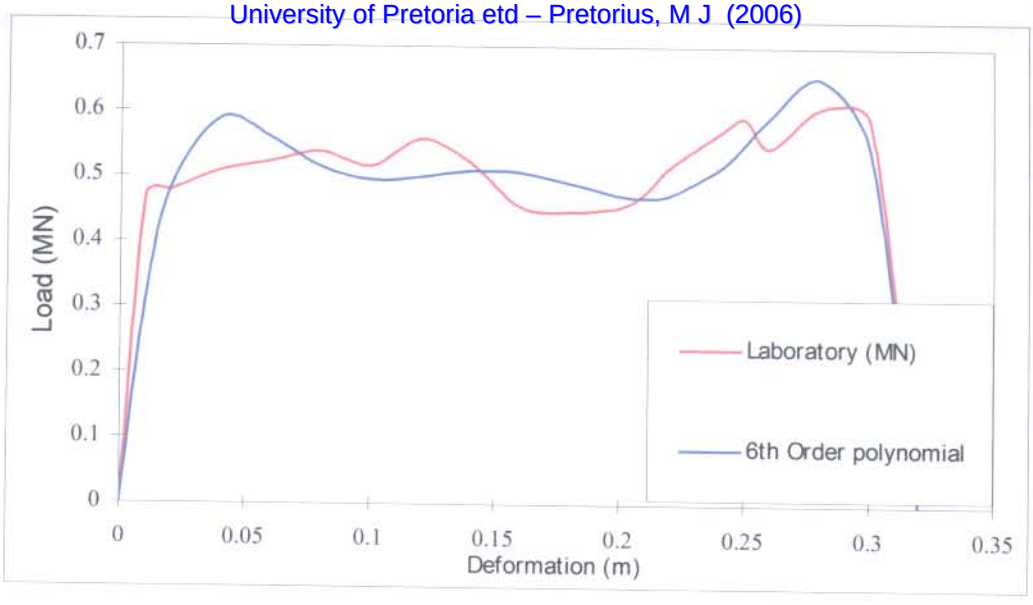

Figure 4.2: Laboratory test results and a 6th order polynomial fit to the data of a 200 mm diameter Wedge Prop, 2.0 m high and tested at a rate of 5 mm/minute

4.3 FACTORS THAT INFLUENCE SUPPORT PERFORMANCE

The following factors influence support performance and require adjustments to the support functions to be made:

4.3.1 Creep

According to Titherington (1970) creep refers to the slow but continuous deformation of a material under a constant stress. The effect of creep manifests in the difference between the support performances of a support element tested in a laboratory compared to the in-situ performance of the same unit. This comes as a result of the difference in rates of deformation.

Rate of deformation therefore has a major influence on support performance, and must be incorporated in the support function to fully describe and represent the performance of such an element.

The quasi-static underground rate of closure is much lower than the rate at which support units are normally tested. The in-situ performance of a support unit,

expressed in terms of the load generated under this slow rate of closure is lower than laboratory results for the same amount of deformation.

Rapid or dynamic loading has the opposite effect on both timber - and lightweight cementitious support units. In such cases the support unit generates an increased load of resistance when subjected to this higher rate of deformation.

The extent to which the laboratory support performance data must be up- or downgraded as a result of the effect of the rate of deformation, is a function of both material type and the differences between laboratory - and underground rates of deformation.

4.3.2 Height of pack

The taller a pack for the same pack type and base dimensions, the softer it is. This means that the taller pack will generate a lower load at the same amount of deformation than a squat pack with the same base dimensions. The latter is mainly because of an increase in voids, Kotzé (1987), and an increased probability for poor surface contacts between timber surfaces, Spearman and Pienaar (1987) as the slenderness ratio increases.

A method of predicting pack performance from the average contact area between adjacent mats in a pack was developed by Spearman (1983, 1987). The stress-strain relationships derived from pack tests were characterised by straight lines. In his analysis the moduli were correlated with the average percentage contact area of the mats in the packs. Spearman confirmed that the stiffness of the pack is directly related to the contact area.

Correction must be made for this aspect in the design process of support in order to represent the in-situ support reaction as accurately as possible.

4.3.3 Buckling failure of elongate support

Timber elongates tend to buckle and fail when exceeding a critical slenderness ratio. Valuable work has been done in this regard by Roberts, Jager and Riemann (1987) in order to quantify the buckling potential of timber elongate support. This aspect is also incorporated into the mathematical support model.

4.3.4 Pre-stress of support

Stope support is often pre-stressed during installation. This practice forms an integral part of stope support practices underground and influences the support performance at the very early stage during installation. It changes the support behaviour from passive to active as the unit exerts load onto the rockwalls before any deformation of the rockmass has taken place. The pre-stressing of a support element affects the support resistance generated by it on installation.

The support model must include this aspect in order to produce an accurate representation of support performance when quantifying the stope support capacity.

4.4 QUANTIFICATION OF INFLUENCING PARAMETERS

The factors affecting the behaviour and performance of support elements as discussed in 4.3 are expressed in mathematical and engineering terms as follows:

4.4.1 Loading rate factor

This factor describes the effect that the rate of deformation has on the performance of a support unit and compensates for the effect of creep as discussed in 4.3.1. The loading rate factor (Y) is determined for lightweight cementitious packs, timber packs and timber elongates. The effect of the loading rate is discussed under the headings that follow.

(a) Lightweight cementitious packs

A series of results was made available to the author by Smit (1998) of tests conducted by the manufacturer of the lightweight concrete Durapak.® Amongst these results were tests conducted under rapid loading, conventional laboratory tests as well as in-situ results from underground instrumentation.

The rapid loading tests were conducted at the test facility at the Materialprüfungsamt Nordrhein-Westfalen in Dortmund, Germany. The facility can handle up to 650 ton at a maximum loading rate of 400 mm/s. It also has the ability to induce rapid or impact loading at any stage during the test cycle.

This test data is useful and makes it possible to develop a mathematical function that can be applied to the laboratory results in order to calculate the load generated by a support unit for the varying rates of deformation. The adjusted function is developed by applying the adjustment factor to laboratory results until it reproduced the performance curves that were recorded under either quasi-static or rapid deformation rates.

This was done repeatedly on a trial basis and the function continuously changed until the adjusted laboratory results produced a curve similar to the one recorded. The function is developed in a way that it up- or downgrades the performance function of the support unit for various rates of deformation.

Y denotes the load rate adjustment to be made to the support performance function:

$$Y = (1 + {}^{10.4}/_{100})^{-\log(Vo/v)} \qquad (4.2)$$

where:

Y = Loading rate effect adjustment to the support function;
v = Underground rate of closure (mm/minute); and
v_o = Deformation rate of laboratory press test (mm/minute).

A graphical representation of the Y-factor is shown in Figures 4.3(a) and 4.3(b).

The support performance function $y = f(x)$ is multiplied by the Y-factor to compensate for the effect that the rate of deformation has on the performance of the unit. Where $Y>1$, the load generated by the support unit is higher than that generated by the same unit under laboratory conditions. If $Y<1$ the opposite is true and the load generated by the unit will be lower than that under laboratory conditions.

The value for the Y-factor of lightweight cementitious packs is closer to unity for both quasi-static and dynamic loading ranges as illustrated in Figures 4.3(a) and 4.3(b). It is concluded from this that the load rate has less influence on the performance of lightweight cementitious packs than on timber packs or timber elongates.

(b) Timber packs

The rate of loading has a major influence on the support performance of timber support as will be demonstrated and cannot be neglected during the support design process. The force-deformation behaviour of timber packs under rapid loading conditions has not been properly quantified in the past mainly because such a testing facility is not available in South Africa.

Roberts, Pienaar and Kruger (1987) first determined the relationship between the force-deformation behaviour of timber packs underground and the laboratory press. Through this relationship a percentage is calculated with which laboratory results should be reduced to account for the lower rate of deformation underground. This relationship was published as:

$$x = (H_{perp}/H).7\log(v_o/v) \qquad (4.3)$$

where:

x = Percentage reduction in load carried (%);
H = Total height of pack (m);
H_{perp} = Total height of the timber elements in the pack on which the load acts perpendicular to the grain of the timber (m);
v_o = Laboratory rate of deformation (mm/minute); and
v = Underground closure rate (mm/minute).

These findings were extrapolated into an equation that yields the force-deformation behaviour of timber packs at loading rates that will be achieved during expected rockburst conditions of 0.3 m/s to 3.0 m/s. This equation was not verified by laboratory testing at the time because of a lack of a suitable testing facility.

To properly design stope support, it is essential that the support behaviour under rapid loading conditions be accurately quantified. More research has therefore been done in this regard by the CSIR Division of Mining Technology since the first series of tests. Tests were undertaken by the CSIR at the MPA-NRW test facility in Dortmund, Germany by Taggart (1996). The packs were tested at three different loading rates, namely 0.003 m/s, 0.03 m/s and 0.3 m/s. The results of the tests are described by Taggart (1996) who found a linear relationship between a change in deformation rate and the resulting change in pack force of approximately 16 per cent per order of

magnitude change in deformation rate. He also found that the variance is irrespective of the size and the composition of the packs. This relationship is given as:

$$F_{fast} = F_{slow}.\{1+(\%inc/_{100})\}^{\log(Vo/V)} \quad (4.4)$$

where:

F_{fast} = Force at rapid rate of deformation (kN);
F_{slow} = Force at slow rate of deformation (kN);
%inc = Percentage increase in strength (%);
v_o = Fast rate of deformation (m/s); and
v = Slow rate of deformation (m/s).

The previous equation was altered into a format with the ratio F_{fast}/F_{slow} to be consistent to that of the lightweight cementitious packs. This ratio represents the relationship between the forces generated by the in-situ support unit to that of the laboratory unit and is a function of the respective deformation rates.

The Y-factor that describes this ratio is given as:

$$Y = (1+ (^{16}/_{100}))^{-\log(Vo/v)} \quad (4.5)$$

where:

v = Underground rate of closure (mm/minute); and
v_o = Deformation rate of laboratory press test (mm/minute).

Figures 4.3(a) and 4.3(b) show the Y-factor value for timber-, lightweight cementitious packs and timber elongates for both quasi-static and dynamic loading conditions. A factor value 1 indicates a load-deformation performance that is equivalent to the test laboratory results. The analysis demonstrates that the load rate has more influence on the performance of timber packs than on that of timber elongates and lightweight cementitious packs.

The Y-factor varies most from unity in the case of timber packs where the Y-value can be as low as 0.5 for quasi-static conditions to a value of 1.75 under dynamic loading conditions. In practice the in-situ performance of a timber pack under quasi-static conditions can therefore be as low as 50% of the laboratory test results. For dynamic

loading conditions of say 3 m/s this value can be as high as 1.75. This means that the pack will generate a load of 75% more than that of the laboratory test results.

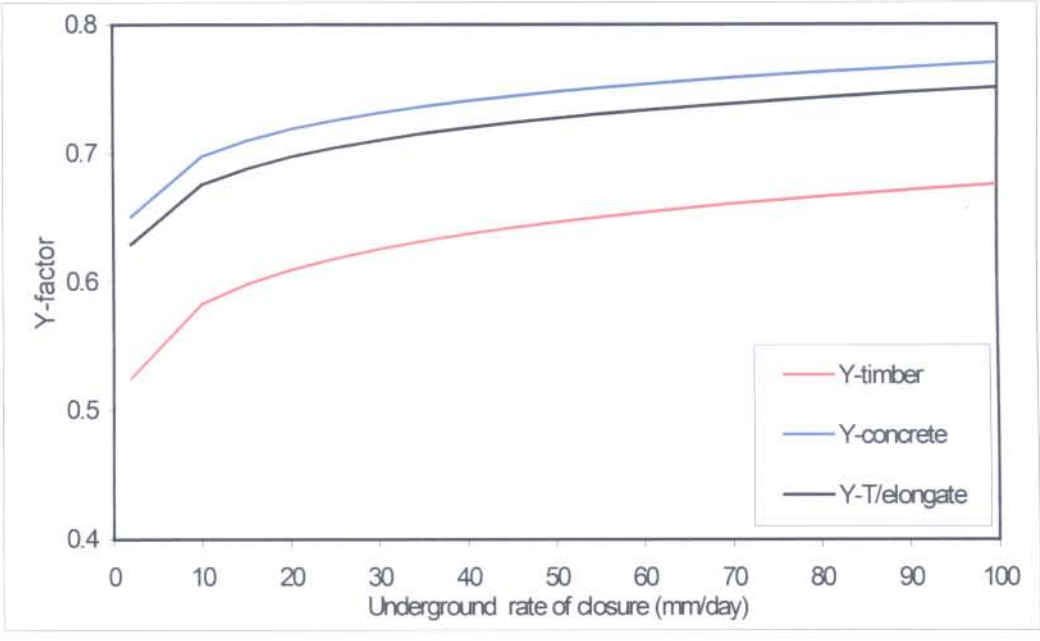

Figure 4.3(a): Y-factor values for timber-, lightweight concrete packs and timber elongates for quasi-static loading conditions

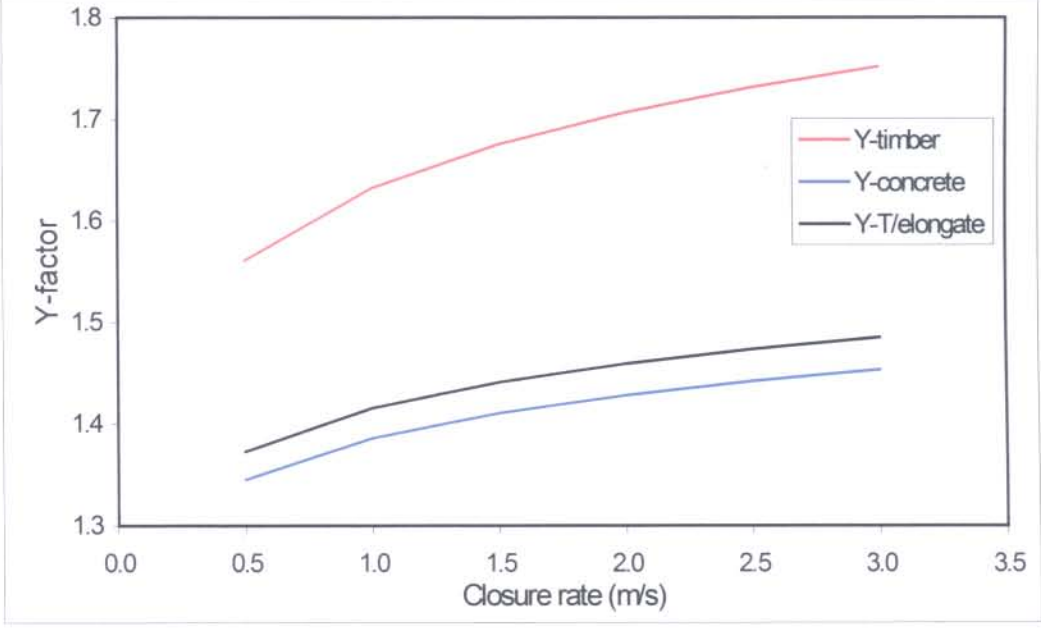

Figure 4.3(b): Y-factor values for timber-, lightweight concrete packs and timber elongates under rapid loading conditions

(c) Timber elongate support

The force-deformation curves can be adjusted up- or downward to account for different loading rates. This is done according to data published in this regard by Roberts (1987) as shown in Figure 4.4.

For example the logarithm of the two differing loading rates is taken and the force correction factor is read off the graph shown in Figure 4.4. If a force-deformation curve was determined in a laboratory test at 40 mm/minute and it is required to know the force-deformation behaviour of the unit under a stope closure of 10 mm/day, then:

$\log(v_o/v)$ = log(40 mm/minute/10 mm/day)
= log(57600 mm/day/10 mm/day)
= 3,76

Reading the force correction from the graph indicates that the force should be multiplied by a factor of 0,76. This will result in a reduced force exerted by the unit of approximately 76% of that of the laboratory test.

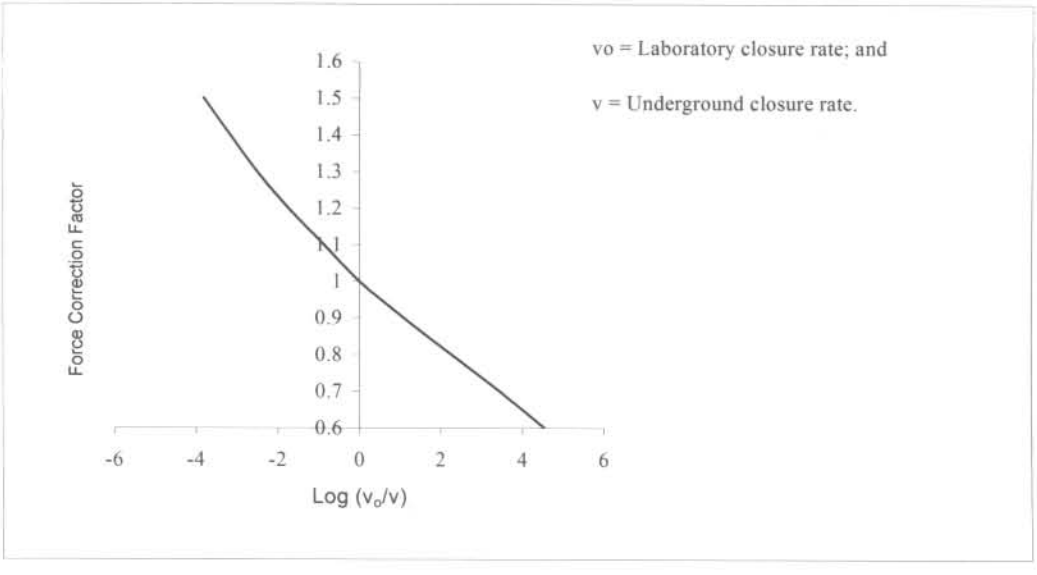

Figure 4.4: Force correction factor for timber elongates as developed by CSIR

This curve is represented mathematically in a format that allows it to be integrated with the support performance functions. Adjustments can be made from this to the support

performance function of timber elongated type of support. The equation that describes the force correction factor is given by:

$$Y = c_{e1}.[\log (v^o/_v)]^2 - c_{e2}.[\log (v^o/_v)] + 1 \quad (4.6)$$

where:

Y = Loading rate effect adjustment to the support function;
v = Underground rate of closure;
v_o = Deformation rate of laboratory test;
c_{e1} = 5.3E-3; and
c_{e2} = 0.1084

Figure 4.5 illustrates how well the Y-factor quadratic equation describes the force correction curve that was developed by the CSIR.

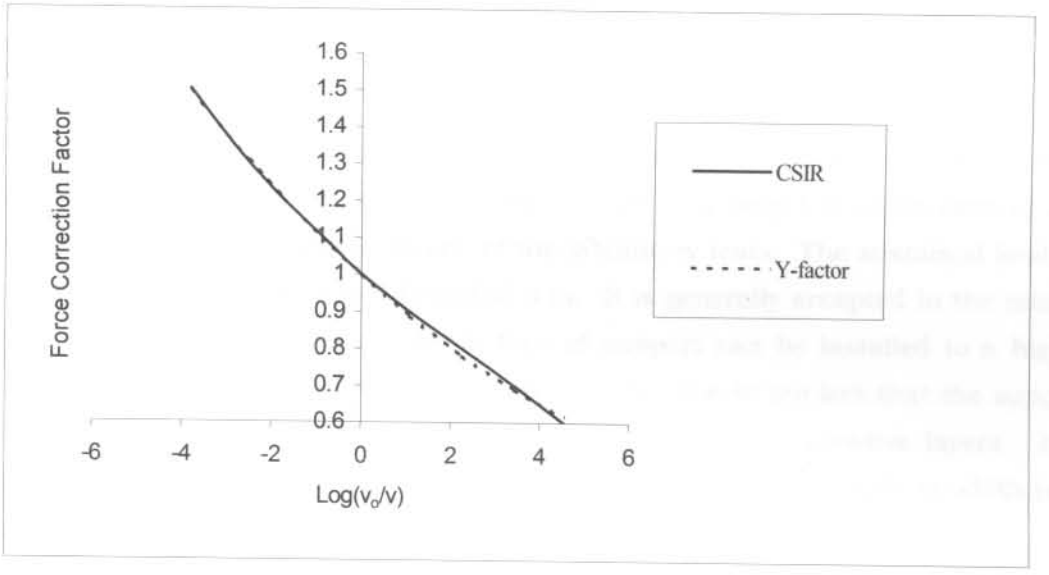

Figure 4.5: Correlation between quadratic Y-factor equation and curve developed by the CSIR

Figures 4.3(a) and 4.3(b) show the Y-factor value for timber-, lightweight cementitious packs and timber elongates for both quasi-static and dynamic loading conditions. The Y-factor for timber elongates varies less from the value of 1 than when compared to the results of a timber pack.

It shows that the Y-factor value can be as low as 0.62 for quasi-static loading conditions to a value of 1.45 under dynamic loading. This means that a conventional timber elongate unit will only be able to generate 62% of the laboratory test results under quasi-static loading conditions. It can however generate as much as 45% more load in-situ than in the laboratory during rapid deformation at a rate of say 3 m/s.

4.4.2 Support height factor

The influence that the height of a support unit has on the performance of both lightweight cementitious - and timber packs is described in 4.4.2(a) and (b).

(a) Lightweight cementitious packs

A number of laboratory test results that were done on different heights of packs were used for the purpose of this analysis. The sustained load of the different heights of packs are determined and plotted against the height of the pack. This relationship is described by fitting a mathematical function to the data.

The base dimension of the packs tested were 60 cm x 60 cm and the packs were constructed to a height of 180 cm. The latter relates to a height to width ratio of 3:1. No buckling failure was observed in any of the laboratory tests. The sustained load for taller packs was extrapolated to a height of 3 m. It is generally accepted in the mining industry that a lightweight cementitious type of support can be installed to a higher height to width ratio than conventional timber support due to the fact that the support matrix is homogeneous with firm and total contact between successive layers. It is expected that buckling failure will start taking place once a certain height to width ratio is exceeded, but no literature could be found that defines this upper limit.

It is established that the best way of predicting pack performance using the height factor (H_f) for lightweight cementitious packs was through the ratio of two fifth order polynomial functions. The height factor for a lightweight cementitious pack is given by the ratio of the functions of the pack installed underground to the one tested.

$$H_f = y_{sw}/y_{th} \qquad (4.7)$$

where:

H_f = Height factor adjustment to the support performance function;

y_{sw} = 5th Order polynomial for the pack height (x_1) underground unit;

$= c_1x_1^5 + c_2x_1^4 + c_3x_1^3 + c_4x_1^2 + c_5x_1 + c_6$

x_1 = Stoping width or underground pack height (m);

y_{th} = 5th Order polynomial for the pack height tested in the laboratory;

$= c_1x_2^5 + c_2x_2^4 + c_3x_2^3 + c_4x_2^2 + c_5x_2 + c_6$

x_2 = Height of pack tested in the laboratory (m)

with:

c_1 = -576.24

c_2 = 5956.60

c_3 = -24079.00

c_4 = 47565.00

c_5 = -45937.00

c_6 = 17935.00

Figure 4.6 shows the sustained loads of lightweight cementitious packs for the different pack heights as well as the 5th order polynomial function that represents the data. The analysis indicated that a point is reached at a pack height of approximately 1.25 m where an increase in the height of the pack has hardly any influence on the sustained load of the pack.

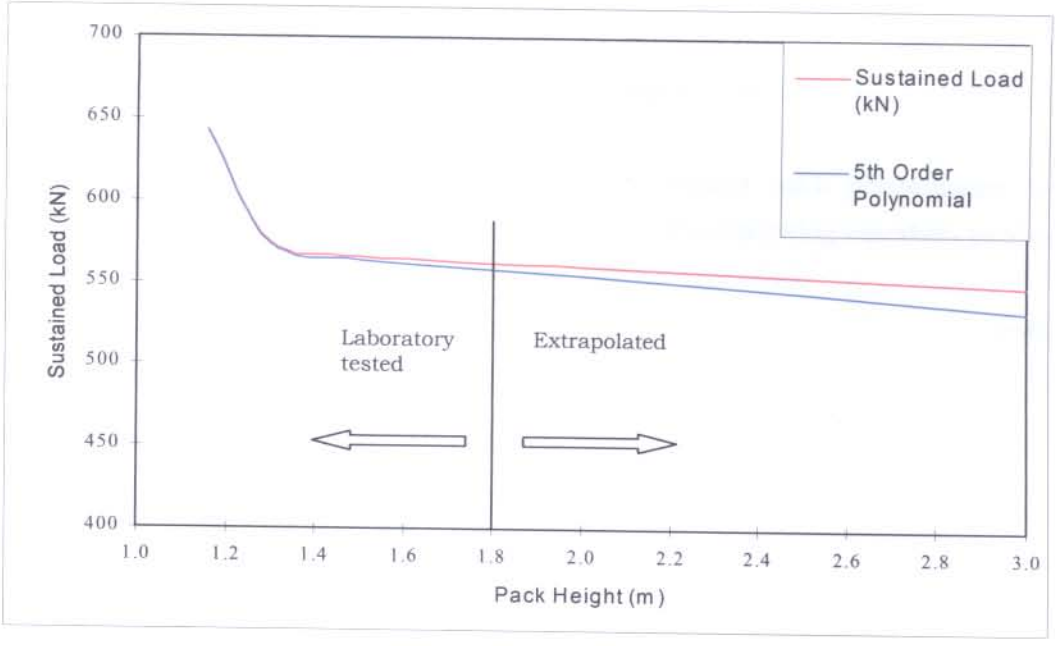

Figure 4.6: Sustained load and mathematical representation of the same data for different heights of lightweight cementitious packs

(b) Timber packs

It is known that the stability of packs decreases with increasing height according to Roberts et al (1995) and Ryder and Jager (2002). It is commonly assumed that timber packs with a height to width ratio exceeding 2:1 are unstable, particularly during dynamic closure. This is a qualitative assessment from underground experience and is assumed to be correct. According to Ryder and Jager (2002) the pack type does have an influence on its buckling potential, with the stiff end-grained types of packs having a higher buckling potential than conventional mat packs.

The pack height adjustment factor is used to adjust the pack performance curve and compensate for the influence that the height of the support unit may have on the performance of the support unit.

A series of tests was done on solid timber packs at different heights but with the same base dimensions. The objective is to develop a correction factor (H_f) to be applied to compensate for the difference in height. Such a function must ideally be able to account for the continuous change in width to height ratio of the support unit during the deformation process.

Tests were conducted on solid timber packs with base dimensions of 0,75 m x 0,75 m and heights of 0.9 m, 1.1 m, 1.3 m and 1.5 m. From these results a number of factors were developed to account for the differences in the support performance.

A number of different equations were developed to predict pack performance for a different pack height from an existing or known pack. The following equation produced the best fit to the pack performance curve it is intended to predict.

$$H_f = (T_h/S_w).(1+[(D_{ef}/S_w) - (D_{ef}/T_h)]) \quad (4.8)$$

where:

T_h = Height of pack tested (m);
S_w = Stoping width (m); and
D_{ef} = Deformation (mm)

Figure 4.7 shows a typical application of this principle where the original test curve of a 1.1 m pack is plotted. It shows the prediction of a 1.1 m high pack curve extrapolated from data of the 1.5 m, 1.3 m and 0.9 m high packs respectively.

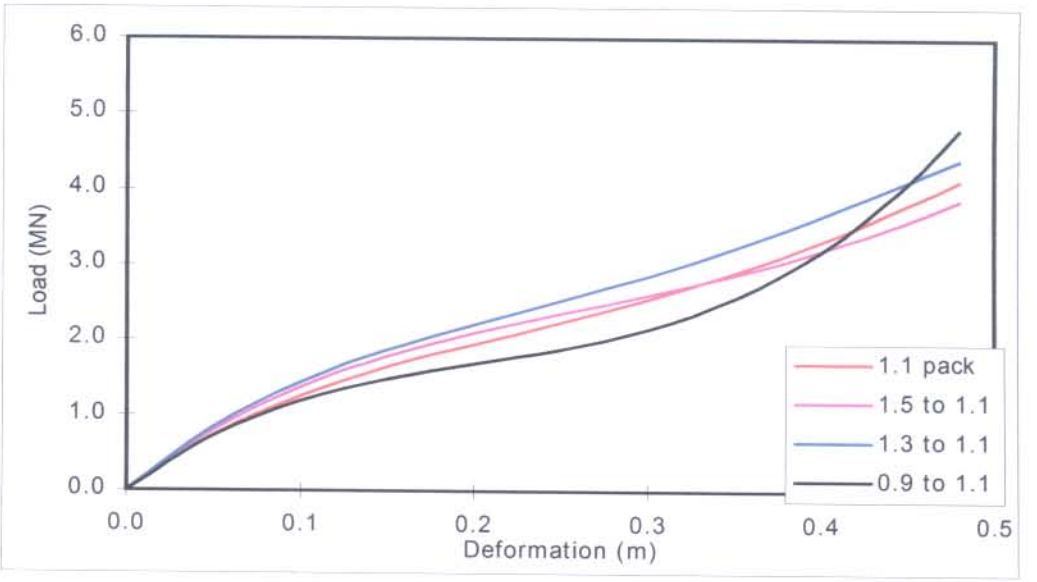

Figure 4.7: Prediction of a 1.1 m high solid matpack from data of 1.5 m, 1.3 m and 0.9 m high packs

It was accepted that this approach yields an adequately accurate representation of the load-deformation curve of a timber support unit that is predicted from the performance curve of a pack of the same type.

4.4.3 Buckling failure of timber elongate support

Buckling failure of an elongate has a major impact on the design of support since it influences the stability of the unit once a certain amount of deformation is exceeded. Buckling failure of elongate support does not only affect the ability to absorb energy but also the stiffness of the unit during deformation.

Props with an increased yield range have a higher energy absorption ability or capacity. According to Roberts (1991) high closure prior to the event reduces the ability of a yielding timber elongate to absorb energy during a rockburst.

The factor applied to account for buckling failure of elongate support is given below. Here the elongate support performance function is adjusted to represent the typical performance of an elongate under buckling failure conditions.

$$B_f = 1 - (S_w - 1).10^{(10x-2)} \qquad (4.9)$$

where:

B_f = Buckling failure factor of elongate;

S_w = Stoping width (m); and

x = Deformation (m)

Note that:

for a stoping width $S_w < 1$ m, $B_f = 1$, and

for stoping width $S_w > 2.5$ m, $B_f = 0$

The effect that buckling failure has on the performance of a typical elongate is illustrated by Figure 4.8. The laboratory test result shows a 160 mm diameter Profile Prop, 1.0 m long that was tested at a rate of 10 mm/minute. The adjusted curve represents the effect of buckling of the same support element that is installed at a height of 1.8 m with an underground closure rate of 10 mm/day. This illustration shows that the buckling of the support unit does not only affect the peak load generated by the longer unit but also that it has shed all load at a deformation just over 200 mm as opposed to the 500 mm in the test press. The stiffness of the in-situ unit is also different to the laboratory test result.

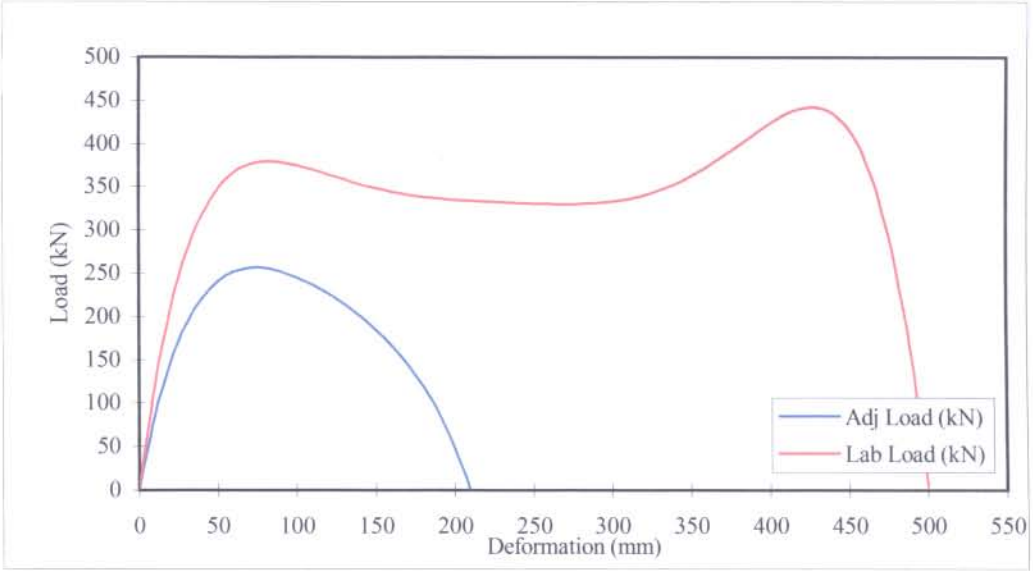

Figure 4.8: Effect of buckling on the performance of a 160 mm-diameter Profile Prop

4.5 ADJUSTED MODEL

All factors that influence the performance of a support unit are incorporated into a single mathematical equation to get an all-inclusive support performance model.

These factors are introduced and integrated in an adjusted support function. This function describes the in-situ performance of stope support elements. It represents its support performance for both quasi-static and dynamic loading conditions. It is given for the following support groups:

4.5.1 Pack support performance function

The adjusted function for pack support is described by the support performance function $f(x)$ that is adjusted to compensate for the rate of deformation (Y) and height influence (H_f). The adjusted support performance function $f_a(x)$ for pack support is given by:

$$f_a(x) = f(x).Y.H_f \qquad (4.10)$$

where:

$f_a(x)$ = Adjusted support function for pack support;
$f(x)$ = Function describing the support performance of a specific pack type (timber & lightweight cementitious material);
Y = Loading rate factor as described in 4.4.1 (a) and (b); and
H_f = Support height factor as described in 4.4.2 (a) and (b).

4.5.2 Timber elongate support performance function

The adjusted support performance function for elongated support is similar to that of the packs with the difference that a buckling factor B_f is introduced in the function. The adjusted support performance function is thus given as:

$$f_a(x) = f(x).Y.B_f \qquad (4.11)$$

where:

$f_a(x)$ = Adjusted support function for timber elongates;
$f(x)$ = Function describing support performance of a specific timber elongate; and
Y = Loading rate factor as described in 4.4.1(c); and

B_f = Buckling failure factor for elongate as described in 4.4.3.

4.6 OUTPUT FROM THE ADJUSTED SUPPORT MODELS

The adjusted stope support performance function embodies information that is relevant to the design of stope support. Once the stope support performance function is presented in the format as shown in 4.5.1 and 4.5.2 the function can be applied mathematically to produce the following as output:

4.6.1 In-situ load

The in-situ load generated by a support unit is determined by substituting the deformation value of interest (x) into the adjusted function $f_a(x)$ for the specific support element. The load generated by the support element represents its actual or in-situ performance and takes into consideration all factors that influence its performance.

Figure 4.9 shows both the laboratory test press results as well as the in-situ load generated by a 75 cm x 75 cm Brick Composite pack. The pack is 1.5 m high and was tested at 30 mm/minute while an underground closure rate of 20 mm/day is simulated.

The effect that the slow deformation rate has on the support performance is illustrated.

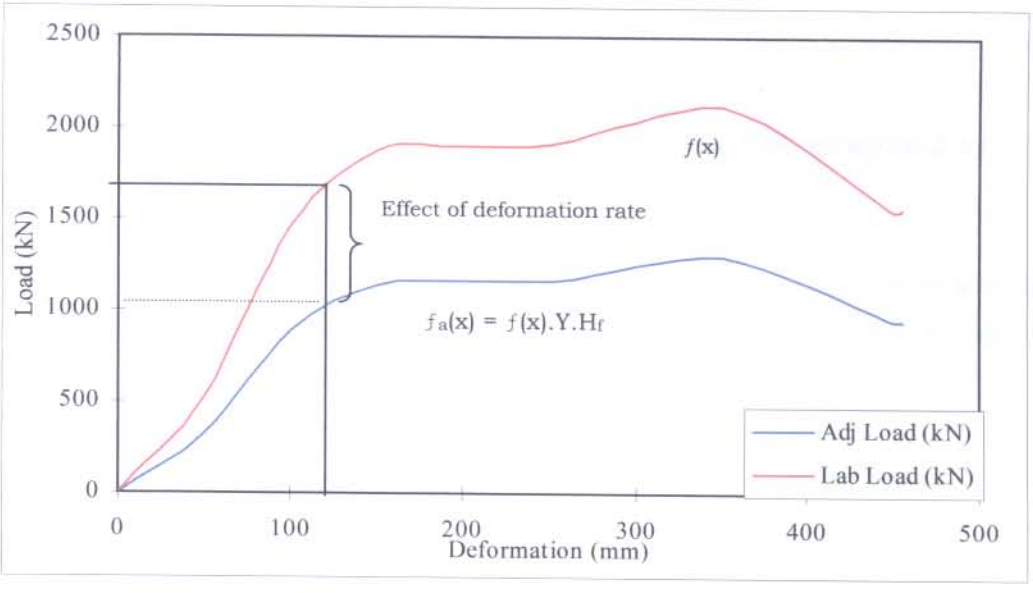

Figure 4.9: Laboratory and in-situ support performance of a 75 cm x 75 cm 9-Pointer Brick Composite pack

Figure 4.10 shows the effect that the buckling failure has on the support performance of a 160 mm diameter Profile Prop of 1.0 m high that was tested at 10 mm/minute. It illustrates the effect that buckling failure has on the load generated by the elongate. The underground unit that is simulated is 1.8 m in length with an underground closure rate taken at 20 mm/day.

The analysis demonstrates that total failure of the 1.8 m long Profile Prop has taken place after 210 mm of deformation. The laboratory test results of the 1.0 m long unit show that final failure starts to occur at approximately 450 mm deformation.

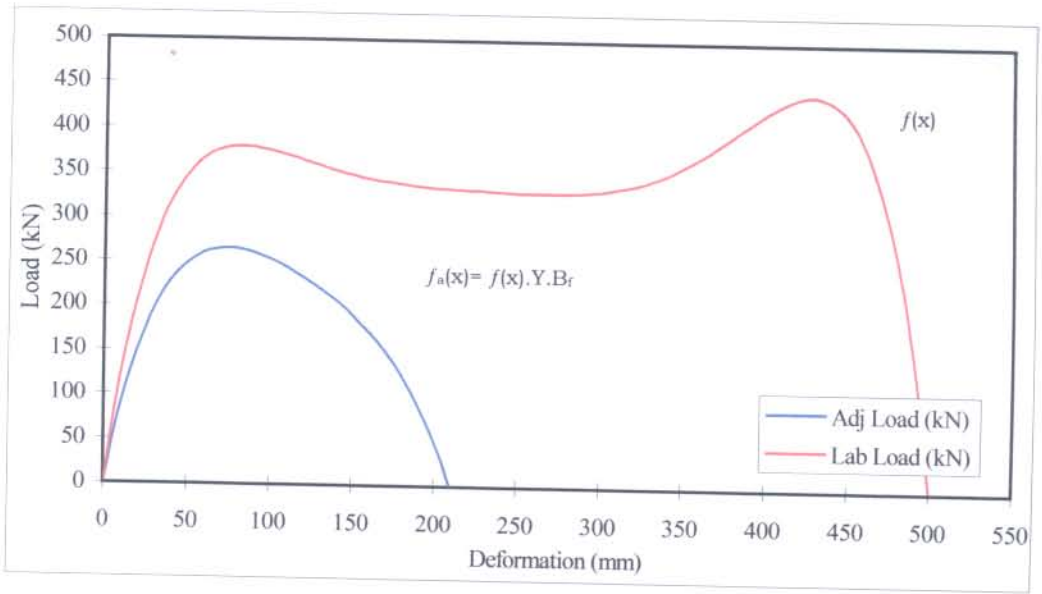

Figure 4.10: Effect of loading rate and buckling on the load generated by a 1.8 m long 160 mm diameter Profile Prop

Figure 4.10 illustrates that the in-situ load generated by the taller support unit for the same amount of deformation is less than that of the laboratory test results of the shorter one.

The analysis also demonstrates that the factors influencing its performance do not only have an impact on the stiffness of the support element but also on its energy absorption capacity as discussed in 4.6.3 and 4.6.4.

4.6.2 Support resistance

The support resistance (SR) of a unit is defined as the load generated per unit area for a given amount of deformation. It is assumed that a tributary area is allocated to a support unit. The tributary area is calculated as the product of dip - and strike spacing of the support. Support resistance is expressed in kilonewton per square meter, (kN/m^2).

The support resistance at the given point of deformation is calculated by dividing the load generated by the support unit by its tributary area. Support resistance is given as:

$$SR = f_a(x)/(D_s.S_s) \quad (4.12)$$

where:

SR = Support resistance (kN/m^2);
D_s = Dip spacing of support elements (m); and
S_s = Strike spacing of support elements (m).

4.6.3 Stiffness of support unit

The slope of the load-deformation curve represents the stiffness of the support element. Stiffness of a support unit is defined as the change in load generated per unit deformation and expressed in kN/mm. Stiffness also indicates strain hardening or softening of the support.

Stiffness of the support unit at any point of deformation is determined by differentiating the adjusted support performance function. It is calculated mathematically as $\partial/\partial x[f_a(x)]$ for any point (x) of deformation.

The stiffness of the support unit is given as $\partial/\partial x[f_a(x)]$ where $f_a(x) = f(x).Y.H_f$ for packs and $f_a(x) = f(x).Y.B_f$ for timber elongates. The combined function is differentiated as the product of two functions $f(x)$ and B_f (Buckling failure - elongates) or H_f (Height factor – packs) all functions of deformation x.

The adjustment functions are defined as given in 4.3 of this chapter namely the factors that influence support performance.

This concept is further illustrated in Figure 4.11 that shows the same load-deformation curve of the laboratory and in-situ Brick Composite packs presented in Figure 4.9.

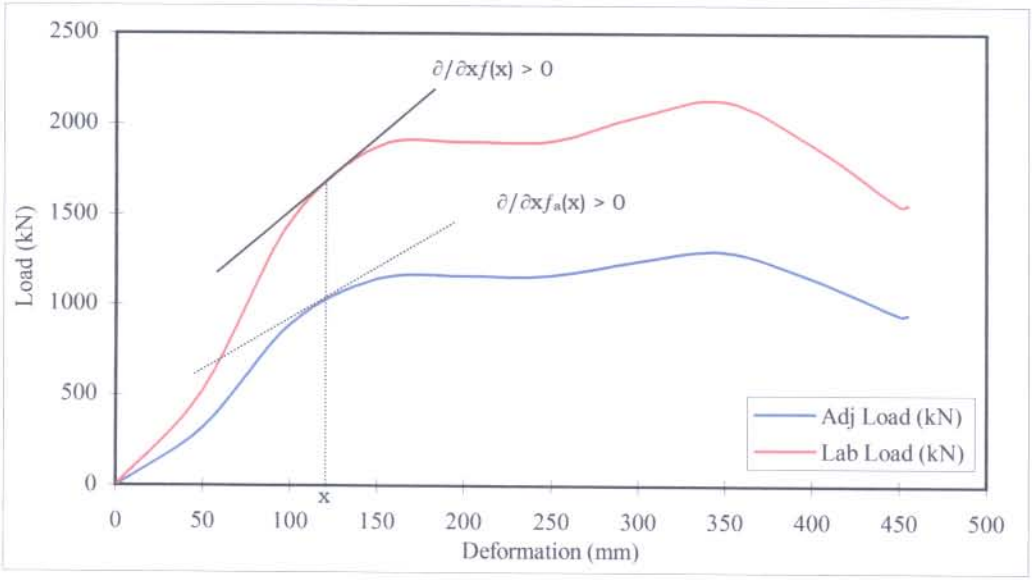

Figure 4.11: Difference in stiffness of the 75 cm x 75 cm Brick Composite pack for laboratory and in-situ performance functions

Figure 4.11 illustrates how the in-situ stiffness of an elongate can be different from the laboratory results for the same magnitude of deformation. The quasi-static underground rate of deformation is taken as 20 mm/day as opposed to a laboratory test rate of 10 mm/minute that is simulated.

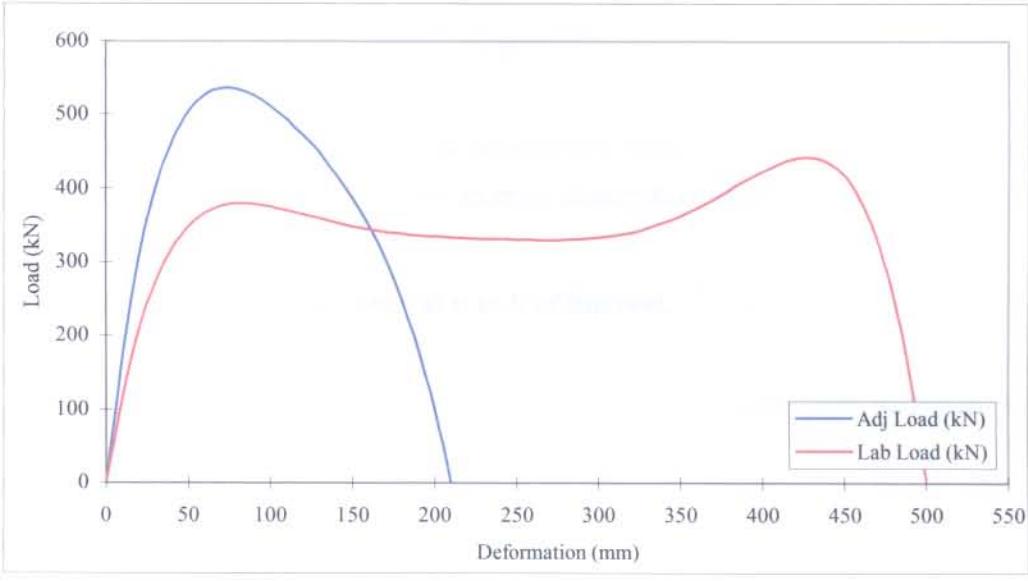

Figure 4.12: Effect of the rate of deformation and buckling of the elongate on the performance of a 160 mm diameter Profile Prop

Figure 4.12 illustrates that this is also true in the case of rapid deformation of the same unit. The curves that are produced show results of a Profile Prop 1.8 m in length, deformed at a deformation rate of 1 m/s as opposed to a laboratory test of the same unit of 1.0 m in length that was tested at 10 mm/minute. It illustrates how the rate of deformation can influence the stiffness of the support unit through the entire range of deformation.

The following data can be determined and quantified from the support stiffness analysis:

1. The magnitude of strain hardening and/or softening of a support unit at any given point of deformation as expressed in kN/mm, and
2. The point of where failure or strain softening starts occurring for any support type i.e. where $\partial/\partial x[f_a(x)] = 0$

4.6.4 Energy absorption capacity

As the rate of deformation influences the load generated by the support unit and likewise its stiffness, this will also have a direct influence on the energy absorption capacity of that particular support unit. The same is true for the underground height of

installation as opposed to the height of the unit tested. This also has an influence on the support performance of an element and therefore its capacity to absorb energy.

The energy absorbed by the support is determined mathematically by integration of the adjusted support function $f_a(x)$. The energy absorption capacity that is expressed in kilo-joule (kJ) is determined as:

$\int_a^b f_a(x)\partial x$ for the deformation interval a to b of interest.

This principle is illustrated for a 75 cm x 75 cm Brick Composite pack in Figure 4.13.

The following rule of partial integration applies when calculating the energy absorption capacity of a support unit:

$\int_a^b f_a(x)g(x)\partial x = f(x).\int_a^b g(x)\partial x - \int_a^b [\int_a^b g(x)\partial x] f'(x)\partial x$ with the functions $f_a(x)$ and $g(x)$ as defined.

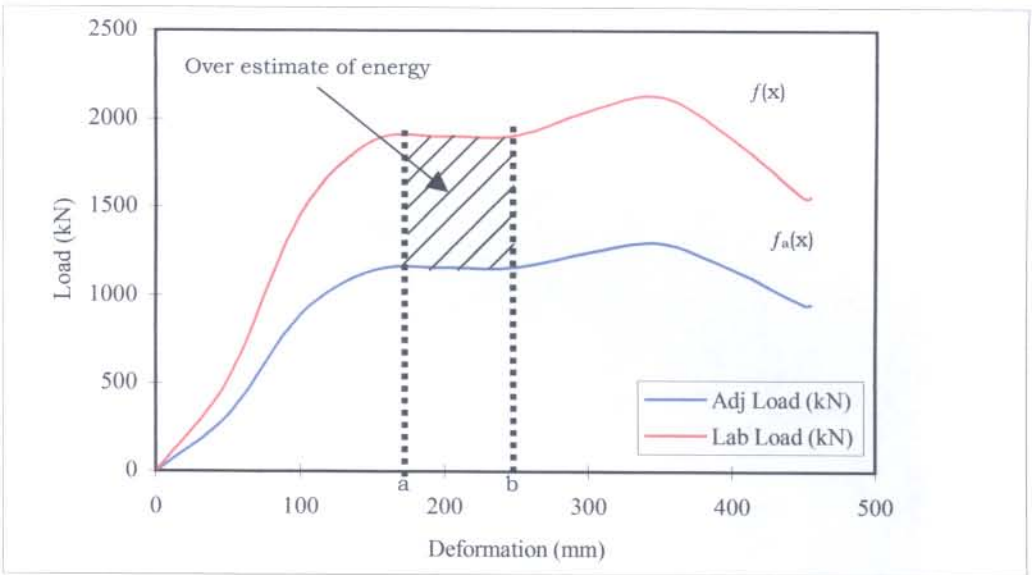

Figure 4.13: Effect of the rate of deformation and height of support on energy absorption capacity of a 75 cm x 75 cm Brick Composite Pack

4.6.5 Stress exerted onto hangingwall during quasi-static and dynamic loading

Current design of stope support during dynamic loading evaluates the stope support type based on the remaining energy absorption capacity of the support element. (Roberts (1995) - SIMRAC GAP032 Final Project Report.) The energy absorption capacity of a support element is calculated as the difference between the total energy capacity (prior to any deformation) and the amount of energy absorbed by the support element at the point of dynamic loading.

Damage often occurs to the stope hanging- or footwall during dynamic loading of the support in rockburst conditions or where the support spacing is too wide. Support may cause the excavation walls to fail around the support element if the load transferred to the walls exceeds its strength. In certain instances the support units suffer very little or no permanent damage at all.

A typical example of the previous statement is illustrated in Figure 4.14 where Hercules type of pack support was used. It shows stope hangingwall damage after a rockburst that measured 3.1 on the local magnitude scale at Unisel Shaft on Harmony Gold Mine in the Free State Gold Fields. The base dimensions of the packs are 75 cm x 75 cm with a stope width of approximately 150 cm prior to the rockburst.

Figure 4.14: Damage to a stope hangingwall during a rockburst with a stiff type of permanent stope support

The stress generated by the support element and exerted onto the hangingwall during dynamic loading and deformation is important during the evaluation of a stope support system. This information can be used once the strength of a fractured stope hangingwall plate under dynamic conditions is fully understood and quantified.

The stress exerted onto the hanging- and footwall is calculated as:

$$\sigma_h = f_a(x)/A_p \qquad (4.13)$$

where:

σ_h = Stress exerted onto excavation walls by the support element (MPa);

$f_a(x)$ = Adjusted support function; and

A_p = Support/excavation wall contact area (m^2).

4.7 OTHER APPLICATIONS

During the development of the stope support model it became evident that it is possible that an estimate of the support resistance generated by a stope support system be determined. This is possible through the application of a pseudo three-dimensional elastic numerical model like Minsim W.

The Minsim W program has a feature where the user can define his/her own variable in the benchmark listing. The advantage of this or a similar model is that it makes it possible that a stope face configuration can be modelled, regional support incorporated, and support resistance calculated and contoured. One support type can be compared to another for the same underground layout and rate of closure through this approach. Areas with an insufficient support resistance as a result of say leads or lags can be identified and additional support introduced where required.

The Minsim W assumes the rockmass to be homogeneous, isotropic and elastic. To compensate for the inelastic deformation of the rockmass the Modulus of Elasticity is modified so that calculated elastic closure relates more closely to that observed underground. It must be noted that this only represents an estimate of the in-situ closure and must be interpreted as such.

To test the above, an area was modelled using Minsim W and the convergence at the centre of the panel calculated and compared to various underground closure rates in

mm/m face advance. This was done in mining steps in order to estimate values for the Young's modulus.

A constant face advance of 1 m per blast was assumed for the calculation for different underground rates of closure. The Young's modulus in the program was altered until the numerical analysis reproduces the same convergence at the centre of the panel as the inelastic or in-situ stope closure.

The layout modelled with leads, lags and limited spans is shown in Figure 4.15. Poisson's ratio was taken as 0.2 with horizontal virgin stress 50% of the vertical while a stope width of 1.5 m was modelled.

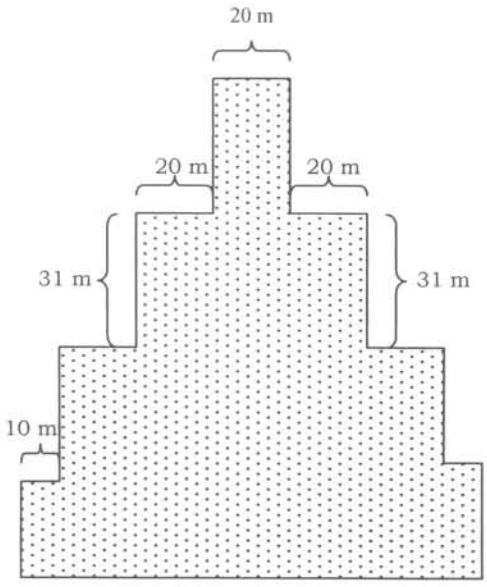

Figure 4.15: Schematic layout of area modelled for determining the modified Young's modulus

Table 4.1 gives a summary of the Young's Modulus that was obtained to reproduce the underground closure rates as shown.

Table 4.1: Modified Young's Modulus for different closure rates

Closure rate (mm/m face advance)	Young's Modulus (MPa)
1	56193
10	5619
20	2810
30	1893

Any formulae can be introduced as a so-called OWN variable in Minsim W in order to calculate that what the user defines. The variable that was introduced in this case to calculate support resistance generated by a support system is given as:

$$OWN = f_a(s_z - s_n)/(D_s.S_s) \quad (4.14)$$

where:

OWN = Support resistance generated by the support system (kN/m²);

$f_a(x)$ = Adjusted support functions compensating for the variables listed;

s_z = Elastic convergence calculated by Minsim W (mm);

s_n = Convergence that has taken place prior to the installation of the support at an installation distance n-meters from the stope face (mm);

D_s = Dip spacing of support elements (m); and

S_s = Strike spacing of support elements (m).

Figure 4.16 demonstrates the application of this methodology. It shows the support resistance contours generated by a 110 cm x 110 cm Hercules timber pack with an underground closure rate of 30 mm/m face advance. The packs are installed at a spacing of 3.0 m by 4.0 m at a stoping width of 1.5 m. The dip of the reef was modelled flat at 0°. The Young's modulus used in the numerical model in this case is 1893 MPa.

The other input parameters for the model are as follows:

Vertical virgin stress gradient:	0.0270 MPa/m
Horizontal virgin stress gradient:	0.0270 MPa/m
Poisson's ratio (ν):	0.2
k-ratio:	1.0
Mining depth:	1000 m
Grid size:	10 m

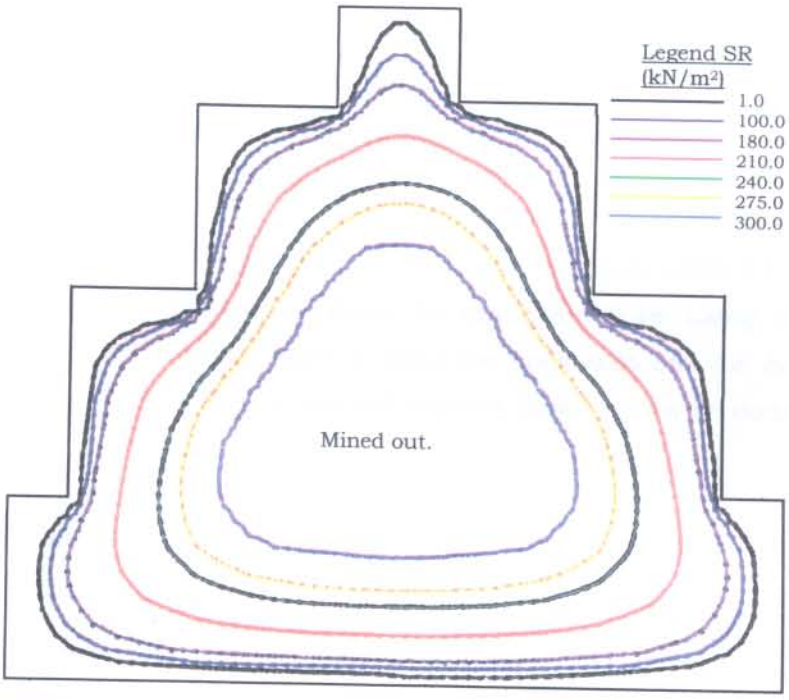

Figure 4.16: Support resistance contours of 110 cm x 110 cm Hercules type timber packs

It is possible that those areas can be identified where there is a lack of support resistance generated by the specific support type at the given support spacing. These areas developed as a result of leads and/or lags between panels for the layout that was modelled. Additional support in the form of temporary support can be introduced to compensate for this.

The stress exerted onto the hangingwall for any mining configuration can be determined in the same way. The area where the stress exerted or transferred onto the rockwalls exceeds the strength of the hanging- or footwall can be identified through this. The variable to calculate stress exerted onto the hanging- or footwall by the support system is given by:

$$\sigma_{rw} = f_a(s_z - s_n)/A_p \qquad (4.15)$$

where:

σ_{rw} = Stress exerted onto rockwalls by the support system (kN/m²);

$f_a(x)$ = Adjusted support function compensating for all the variables defined;

s_z = Elastic convergence calculated by Minsim W (mm);

s_n = Convergence that has taken place prior to the installation of the support an installation distance n-meters from the stope face (mm); and

A_p = Support/hangingwall contact area (m^2).

This methodology can be applied in practice by determining the in-situ closure rate first. An applicable Young's Modulus can be selected from Table 4.1 and the support resistance (kN/m^2) calculated as given by equations 4.14 using the underground support spacing. The stress exerted onto the rockwalls can be calculated by the equation given in 4.15 using the support contact area. It can be done for both quasi-static and dynamic conditions.

4.8 CONCLUSIONS

The study confirmed that it is possible to mathematically represent the laboratory load-deformation behaviour of both pack- and elongate types of support. This mathematical equation can be adjusted in order to compensate for factors affecting support performance such as:

1. Creep;
2. Height of support unit;
3. Buckling failure of elongate support; and
4. Pre-stress of support.

All these factors influencing support performance are also expressed in mathematical and engineering terms, and repeated for both timber and lightweight cementitious support types. The in-situ or adjusted performance function of the support unit captures all the parameters mentioned that influence the performance of the support unit.

This approach proves that it is possible to predict the in-situ behaviour of a support unit where the height of the laboratory test as opposed to the underground unit as well as the laboratory rate of testing and the underground rate of closure are known. The following output can be generated by the adjusted support function:

1. In-situ load generated by the unit;
2. Support resistance of the support;
3. Stiffness of the support unit;

4. Energy absorption of the support unit; and
5. Stress exerted onto the hangingwall.

It was concluded that the outcome of the study could also be used in another application such as calculating the support resistance of a support system through a pseudo three-dimensional elastic numerical model. The use of this approach has much potential where the support resistance for different mining geometries can be contoured and compared as illustrated in this chapter.

REFERENCES

Kotzé T.J. (1987). *Views of the mining industry on timber supports* Proceedings: Mining Timber – From Stump to Stope, South African National Group on Rock Mechanics, June 1987, Pretoria

Roberts M.K.C. (1991). *An evaluation of yielding timber props as a support system in rockburst conditions*, p1-7, Journal of the South African Institute of Mining and Metallurgy, Johannesburg, January 1991.

Roberts M.K.C. (1995). Project Manager: *Final Project Report GAP032, Stope and gully support*, The Safety in Mines Research Advisory Committee (SIMRAC), Johannesburg, Web site www.simrac.co.za.

Roberts M.K.C., Jager A.J. & Riemann K.P. (1987). *The performance characteristics of timber props.* Chamber of Mines Research Report Number35/1987, Johannesburg.

Roberts M.K.C., Pienaar F.R.P. & Kruger F.C. (1987). *Properties of pack supports – comparison of the laboratory and underground performance* p122–135, Proceedings: From stump to stope seminar, South African National Group of Rock Mechanics, June 1987, Pretoria.

Ryder J.A. & Jager A.J. (2002) Editors of: *A textbook on rock mechanics for tabular hard rock mines*, The safety in Mines Research Advisory Committee (SIMRAC), Johannesburg, 2002.

Smit J., Erasmus N. & Grobler R. (1998). *Report on Durapak® design methodology and findings of the rapid load tests conducted in Germany* – March 1998, Internal Grinaker-LTA Report, Johannesburg.

Spearman S.F. & Pienaar F.R.P. (1987). *Compression properties of timber and factors affecting them; performance prediction for packs,* p80–96, Proceedings: From stump to stope seminar, South African National Group of Rock Mechanics, Pretoria, June 1987.

Spearman S.F. (1983). *Improved timber mine supports: Predicting compression behaviour of most packs from contact area between mats.* Council for Scientific and Industrial Research Special Report HOUT 402, National Timber Research Institute, CSIR, Pretoria.

Spearman S.F. (1987). User notes for a computer-based program to predict the performance of mat pack mine supports, National Timber Research Institute, 1987, CSIR, Pretoria.

Taggart P.N. (1996). *Dynamic laboratory testing of pack based support elements. Part 1: The laboratory evaluation of timber and composite packs, single rise elements and pack and grout pre-stressing units.* Internal note: CSIR Division of Mining Technology, August 1994. Journal of the South African Institute for Mining and Metallurgy, Volume 92 No. 2, 1996.

Titherington D. & Rimmer J.G. (1970). *Applied Mechanics,* p144, McGraw Hill Publishing Company Limited, England.

Table 4.2: Constants of polynomials for pack and elongate types of support

Pack Type	Base dimensions (cm x cm)	Height (m)	Lab. test rate (mm/min)	c_1	c_2	c_3	C_4	c_5	c_6
Hercules 4-Pointer	55 x 55	1.37	20	8126.1	-10498	5074.9	-1084.2	84.621	4.0203
Solid Matpack	55 x 55	1.1	5	2781.1	-4572	2852.2	-804.46	91.527	2.632
Hardgum Matpack	55 x 55	1.2	14	-2854.8	4912.2	-3301.7	1137.3	-211.1	25.214
Brick Composite 11R 4-Pt	75 x 75	1.5	10	-128.42	356.73	-389.62	223.58	-75.032	13.635
Brick Composite 9-Pointer	75 x 75	1.5	30	30968	-44757	24333	-6078.8	644.98	-9.3052
Hercules 16-Pointer	75 x 75	1.87	20	2781.4	-4995.1	3306.9	-958.77	94.045	10.365
Sandwich Pack	75 x 75	1.4	10	-5188.8	11435	-9383.5	3503.6	-587.17	44.556
Solid Matpack	75 x 75	1.5	15	626.05	-2310.3	2347	-989.28	178.35	-3.8152
Hardgum Matpack	75 x 75	1.8	14	759.77	-1636.4	1306.8	-440.47	40.768	13.918
Solid Timber	75 x 75	1.4	10	427.86	-225.73	-292.15	311.73	-106.37	18
Timber Composite 9-Pointer	75 x 75	1.5	10	1440	-3144.7	2575.6	-942.79	126.57	9.4529
Brick Composite 11R 16-Pt	110 x 110	1.58	16	15473	-26035	16851	-5120.8	675.86	-9.7696
Brick Composite 11R 9-Pt	110 x 110	2.0	25	96.953	-271.62	262.79	-86.164	-13.601	15.228
Brick Composite 10R 9-Pt	110 x 110	2.2	10	-43.106	151.39	-209.03	150.11	-61.66	15.759
Brick Composite 10R 16-Pt	110 x 110	2.5	20	-8.3346	36.128	-60.162	57.564	-39.383	17.552
End-grain Pack 14R	110 x 110	2.2	10	1126.8	-2074.6	1238.1	-201.18	-53.074	24.204
Hercules Pack	110 x 110	1.7	15	31034	-41715	20367	-4099.6	180.59	45.113
Sandwich Pack	110 x 110	1.7	10	29810	-42212	21796	-4878.3	387.64	25.66
Skeleton 16-Pointer	110 x 110	2.1	10	-10.627	49.947	-86.411	78.193	-37.171	11.668
Solid Matpack	110 x 110	1.8	10	307.11	-971.74	915.69	-294.17	-2.5418	23.83

Pack Type	Base dimensions (cm x cm)	Height (m)	Lab. test rate (mm/min)	c_1	c_2	c_3	c_4	c_5	c_6
Hardgum Matpack	110 x 110	2.5	14	-6646.2	7935.4	-2611.4	-163.57	187.37	-1.1599
Solid Timber Pack	110 x 110	1.7	10	21631	-32122	18076	-4646	481.49	11.69
Solid Timber Pack	110 x 110	2.0	10	1632.9	-3584.7	2921	-1044.4	133.33	13.304
Timber Composite Pack	110 x 110	2.0	10	60.777	-195.52	214.86	-77.338	-13.334	15.123
Solid Timber Pack	140 x 140	1.98	14	15622	-25959	16399	-4775.6	575.91	4.1877
Solid Timber Pack	150 x 150	2.0	10	76751	-93801	44431	-9984.8	972.97	4.0109
Durapak	60 x 60	1.15	10	-3054.4	5858.9	-4328	1548.8	-271.12	21.507
Durapak	90 x 90	1.2	10	-3801.3	7774.1	-6106.6	2311.2	-435.93	39.096
Durapak	60 x 90	1.5	20	-1973.7	3929.2	-3081.7	1212.2	-247.46	24.916
Durapak	120 x 120	1.2	10	-4638.2	9409.7	-7425.4	2859.4	-549.74	48.522
Durapak	90 x 120	1.2	10	-3777.6	7579	-5890.8	2248.4	-441.8	42.143
RSS pack	900mm Diameter	1.2	10	-4166.4	2487.8	1253.9	-1070.5	153.76	9.5863
Pambili Pack	630mm Diameter	1.5	15	-132.98	260.79	-180.94	61.823	-21.535	7.3823
Elongate Type	**Diameter (mm)**	**Height (m)**	**Lab. test rate (mm/min)**	c_1	c_2	c_3	c_4	c_5	c_6
Minepole	116	1.8	5	-416899	302132	-82974	10578	-618.23	14.312
Minepole	130	1.2	5	0	4E+07	-9E+06	515888	-11314	91.069
Minepole	130	1.5	5	0	0	0	-47548	1275.3	0.3584
Minepole	132	2.25	5	0	90926	-44174	7410.5	-509.51	13.431
Pencil prop	150	1.8	10	-7568.3	8991.8	-4261.8	1019.7	-131.64	9.5101
Profile prop	160	1.0	10	-4838.9	7048	-4069.2	1190.5	-183.77	13.635
Profile prop	162	1.2	5	-480518	274814	-63834	7772.4	-526.59	19.161

Elongate Type	Diameter (mm)	Height (m)	Lab. test rate (mm/min)	c_1	c_2	c_3	c_4	c_5	c_6
Profile prop	170	1.5	5	0	0	-7488.6	3062.5	-405.69	20.074
Profile prop	180	1.8	10	-35685	45552	-21664	4692.5	-454.58	17.104
Wedge prop	180	1.2	15	-82110	79535	-30070	5606.3	-539.7	25.538
Wedge prop	200	2.0	5	-172561	162641	-59425	10628	-959.25	39.485